

A New Approach based on Wide-Area Fuzzy Controller for Damping of Sub Synchronous Resonance in Power System including DFIG

Y. Bostani, S. Jalilzadeh *

Department of Electrical Engineering, University of Zanjan, Zanjan, Iran.

Abstract- This paper presents the mitigation of subsynchronous resonance (SSR) based on wide-area wide-area fuzzy controller in power systems including a double-fed induction generator (DFIG)-based wind farms linked to series capacitive compensated transmission networks. SSR damping is achieved by adding the fuzzy controller as a supplementary signal at the stator voltage loop of the grid-side converter (GSC) of doubly-fed induction generator (DFIG)-based wind farms. In addition, delays due to communication signals are important in using WAMS. If these delays are ignored, it causes system instability. In this paper, the delays are modeled with a separate fuzzy input to the controller. The effectiveness and efficiency of the WAMS-based fuzzy controller has been demonstrated by comparison with the particle swarm optimization (PSO), and imperialist competitive algorithm (ICA) optimization methods. The effectiveness and validity of the proposed Auxiliary damping control are verified on a modified version of the IEEE second benchmark model including DFIG-based wind farms via time simulation analysis by using MATLAB/Simulink.

Keyword: DFIG, wide-area measurement system, fuzzy controller, subsynchronous resonance

NOMENCLATURE

W_b	Synchronous Speed
T_{wind}	Wind torque
W_t	Wind turbine Speed
P_r	Active power of the RSC converter
P_g	Active power of the GSC converter.
R_s	Stature resistance
R_r	Rotor resistance
T_e	Electric torque of the generator
i_{qs}	Stator's currents in the qd0-frame
i_{ds}	Stator's currents in the qd0-frame
i_{qr}	Rotor's currents in the qd0-frame
i_{dr}	Rotor's currents in the qd0-frame
V_{qs}	Stator's voltages in the qd0-frame
V_{ds}	Stator's voltages in the qd0-frame
V_{qr}	Rotor's voltages in the qd0-frame
V_{dr}	Rotor's voltages in the qd0-frame
ω_b	Synchronous frequency
ω_r	Rotor frequency
ω	Base frequency
f_s	Synchronous frequency
f_n	Natural frequency
f_r	Rotor electrical frequency

1. INTRODUCTION

The problems in the construction of power transmission lines have forced the generating institutions to obtain maximum efficiency from energy transmission lines by methods such as compensation [1]. One method is to compensate the series capacitor. Series capacitive compensation is an important method to improve the transfer capability and transient stability of existing transmission systems. The application of the series capacitor causes an increase in power transmission capacity of the lines, and improvement of system stability. Despite all the advantages it has, the series capacitor causes fluctuations with frequencies less than the nominal frequency of the network, known as SSR [2]. On the other hand, with the increase of wind turbine production capacity and the use of the new generation of these turbines, the production capacity of wind farms has significantly increased [3]. Usually, wind farms are installed offshore, and therefore, long transmission lines are needed to transfer power of wind farm to the power systems. As the length of transmission lines increases, the capacity of the transmission lines decreases, and limited energy can be transmitted from this line. Increasing the capacity of the lines is usually done through series capacitors and reducing the electrical length of the line, which will lead to SSR fluctuations [4]. So far, many

Received: 17 Sep. 2021

Revised: 24 Dec. 2021

Accepted: 27 Jan. 2022

*Corresponding author:

E-mail: jalilzadeh@znu.ac.ir (S. Jalilzadeh)

DOI: 10.22098/joape.2023.9565.1667

Research Paper

© 2023 University of Mohaghegh Ardabili. All rights reserved.

studies, have been done on damping of SSR, that there are two main methods for mitigation of SSR. One method is auxiliary damping hardware. FACTS devices, such as gated-controlled series capacitors (GCSC), thyristor-controlled series capacitor (TCSC), and static var compensator (SVC), can be used to mitigate SSR [17,18]. In addition, the other method is damping control strategies. Sub-synchronous resonance damping control is implemented in grid-side converters (GSC) [19] and control performance of different control signals, including capacitor voltage, current magnitude, and rotor speed, is analyzed. In Ref. [38], the IEEE first benchmark model is adopted for this study, and the superiority of the FOPI based UPFC controller over PI- based UPFC controller is discussed by comparing the results with various performance indices. In Ref. [39], it proposes a powerful fractional-order PI controller to mitigate the subsynchronous oscillations in the turbine-generator shaft due to subsynchronous resonance (SSR) with FACTS devices. In Ref. [40], it explores a robust fractional-order PI (FOPI) controller to diminish subsynchronous resonance (SSR) using a static synchronous series compensator (SSSC). The insertion and fine-tuning of Fractional-order PI controller in the control scheme of SSSC the subsynchronous oscillations are reduced to 4% as compared to conventional PI controller. In Ref. [41], a new approach is proposed for mitigating the problems associated with distance protection by using the synchrophasor measurement. The entire study of simulation is investigated by using a 48-pulse SSSC carried out with the Bergeron model of transmission line in PSCAD. In previous studies, power systems including the IEEE first benchmark and second benchmark SSR studies have been performed on them. This paper uses a power system including the DFIG – based wind farms, which has rarely been seen in previous studies. In addition, WAMS technology has been used in the design of the fuzzy controller. Today, WAMS is widely used in power systems. Since the DFIG – based wind farms are offshore and usually far from the compensated power system and transmission line, using of WAMS is justified [31]. This is important because the auxiliary controller is for SSR oscillation in DFIG controllers, and since this paper used angular velocity, and variations of synchronous generators for auxiliary controller inputs. The Measurement of input quantities in WAMS is done by using phasor measurements units (PMU), which is one of the main components of

WAMS. The important thing is that the delay of signals measured by the PMU should be taken into account in the design of the controller. If this latency is ignored, controller may even cause instability [32]. In this research a fuzzy controller has been proposed to reduce of SSR in power system including DFIG-based wind farms considering time latencies in communication networks. Fuzzy controller had been designed based on Mamdani inference structures. Inputs the fuzzy controller is angular velocity and variations and output is at the stator voltage loop of GSC.

The continuation of this paper consists of the following parts. section 2 describes modeling of IEEE second bench mark DFIG-based wind farms. section 3 offers the definition of SSR phenomenon in series capacitive compensation of transmission lines . section 4 describes designing wide-area fuzzy logic controller based on Mamdani inference system. section 5 discusses time domain simulation end result and section 6 concludes the paper.

2. MODELING OF THE IEEE SECOND BENCH MARK INCLUDING DFIG- BASED WIND FARMS

To evaluate the effectiveness of the new method on auxiliary wide-area fuzzy logic controller, the IEEE second benchmark model, modified by the inclusion of DFIG-based wind farms, is used in Figure 1. As shown in Figure 1, the system has two steam generators with different turbine masses and connected to the infinite bus via a transmission line and a DFIG-based wind farms, which is offshore usually.

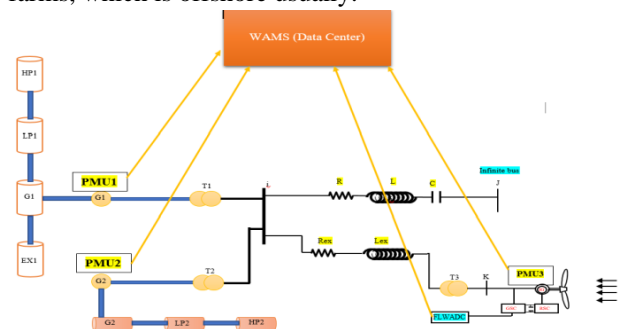


Fig 1. Single Line model of the studied system

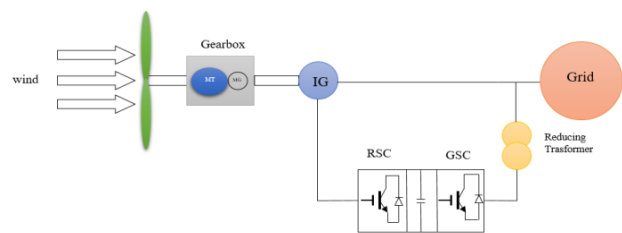


Fig 2. Single Line model of DFIG

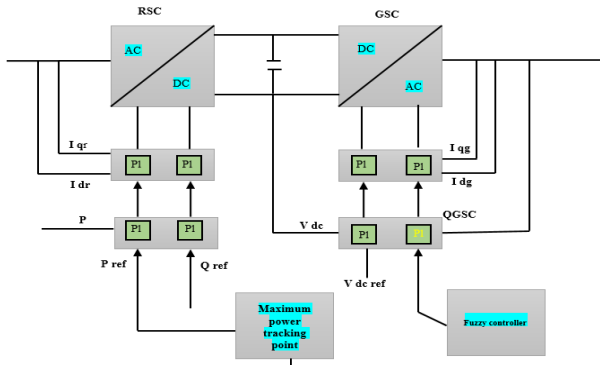


Fig 3.GSC Controller (a) and RSC Controller (b) wind turbine with DFIG

2.1. IEEE Second Benchmark

The standard IEEE second benchmark system has two generators of steam turbine type, each of which has different masses as shown in Figure 1. The first generator is of four masses HP1, LP1, G1, EX1, so it has 3 torsion modes HP1-LP1, LP1-G1 and G1-EX1. The second generator has 3 masses HP1, LP1, G1, which therefore has 2 torsional modes HP1-LP1, LP1-G1 [21].

2.2. Model of DFIG- based Wind Farms

Schematic of DFIG- based wind farms is shown in Figure 2, which has two controllers, rotor-side convertor (RSC) and grid-side convertor (GSC). In addition, two-mass model has been used for the generator turbine shaft system; MT mass for low turbine speed and MG mass for high generator speed, it shown in Figure 2.

In addition, Figure 3 shows the structure of RSC and GSC controllers. According to Figure 3, the RSC controller is used to control the active and reactive power of the converter and the GSC controller is used to control the reactive power and the DC-link voltage between the two converters. According to the references [9], [14], [15], and [16] a wind farm can be modeled as an equivalent wind farm because all the parameters of a wind farm are similar to an equivalent wind farm. The total power is equal to the total installed capacity of wind turbines. For example, a wind farm with fifty 2 MW generators, it is modeled as a 100 MW generator [14].

3. DEFINITION OF SSR

In this part of paper, the consent of SSR is examined. According to the IEEE definition, SSR is a condition in the power system that is associated with the exchange of energy between the electrical network and the generator turbine at one or more natural frequencies of the shaft turbine system below the synchronous frequency [21]. The SSR phenomenon manifests itself in two different

ways, which are: SSR due to steady state and SSR due to transient conditions. In SSR due to steady state frequency subsynchronous, electric currents passing through the armature induce torques and currents in the rotor circuit with f_r frequency equal to:

$$f_r = f_s - f_n \tag{1}$$

In Eq.1, f_s is the synchronous frequency, and f_n is the resonant frequency, which is in Hertz, and obtained from Eq. 2:

$$f_n = f_s \sqrt{\frac{X_c}{X_l}} \tag{2}$$

In Eq. 2, X_c is the compensator reactance and X_l is reactance series of transmission line, both of which are in ohms. The passage of induced currents in the rotor leads to subsynchronous voltage components in the armature, which may in some cases lead to an increase in the subsynchronous armature currents, resulting in self-excitation or steady-state of SSR that divide to induction effect (IG), and torsional interaction (TI). In addition, the other type of SSR occurs in the transient state, when the resonant frequency complement is close to one of the torsional frequencies of synchronous generators [23].

4. MODELLING OF WIDE-AREA FUZZY CONTROLLER IN THE SYSTEM UNDER STUDY

4.1. Review of Fuzzy System

Fuzzy logic is a method of reasoning that is similar to the way humans reason. Fuzzy logic is a type of many-valued logic in which the truth value of variables maybe any real number between 0 and 1. It is employed to handle the concept of partial truth, where the truth value may range between completely true and completely false. Fuzzy logic has four main parts, which are introduced below [33].

Rule Base: It contains the set of rules and the IF-THEN conditions provided by the experts to govern the decision-making system, on the basis of linguistic information. Recent developments in fuzzy theory offer several effective methods for the design and tuning of fuzzy controllers. Most of these developments reduce the number of fuzzy rules.

Fuzzication: It is used to convert inputs i.e. crisp numbers into fuzzy sets. Crisp inputs are basically the exact inputs measured by sensors and passed into the control system for processing, such as temperature, pressure, rpm's, etc.

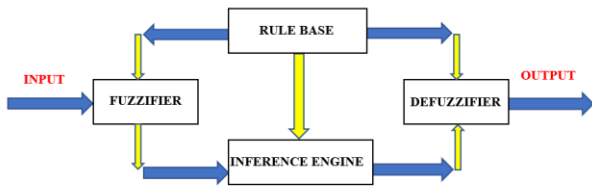


Fig. 4. Fuzzy logic System

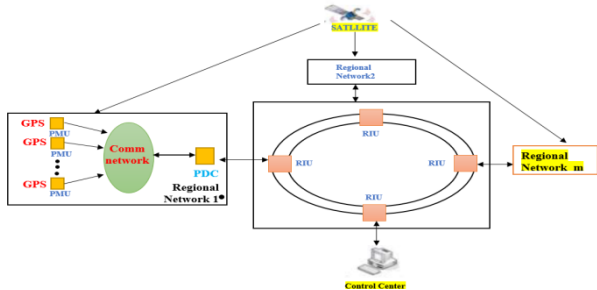


Fig 5. Hierarchical structure of a WAMS

Inference engine: Determines the matching degree of the current fuzzy input with respect to each rule and decides which rules are to be fired according to the input field. Next, the fired rules are combined to form the control actions.

Defuzzification: It is used to convert the fuzzy sets obtained by the inference engine into a crisp value. There are several defuzzification methods available. Centroid technique is one of the commonly used defuzzification methods, is used in this paper.

All of the above are shown in figure 4 [34].

4.2. Review on wide-area measurement systems

By combining the capabilities of telecommunication systems and digital measuring devices and controllers, WAMS enables the monitoring, protection and control of the smart grid over a wide area. In general, WAMS consists of three subsystems, Measurement, telecommunication and processing. The system consists of several (PMUs) and one or more "phase data controllers" (PDCs) connected by a high-speed telecommunications network, figure 5 shows its structure [31].

4.3. Fuzzy controller based on wide-area measurement system

To evaluate the effectiveness of the new method on auxiliary wide-area fuzzy logic controller, used the IEEE second benchmark model, modified by the inclusion of DFIG-based wind farms, is showed in Figure 1. In addition, in Figure 3, indicates the location of the controller based WAMS. In fact, due to the large distance of synchronous generators from wind farms, which are usually offshore, the PMU is used to measure the inputs of the fuzzy system. Damping of SSR is achieved by adding the fuzzy controller as a

supplementary signal at the stator voltage loop of the grid-side converter (GSC) of doubly-fed induction generator (DFIG)-based wind farms. The input signals of this controller are the angular velocity, and variations of synchronous generators, which will have four fuzzy inputs. The fuzzy control output, after being converted to a crisp number obtained by the center of gravity method, is applied to voltage control loop of the GSC. The membership functions for inputs and output of fuzzy controller are obtained, as depicted in Figure 6. In Figure 6, the symbols are defined as NL: negative large, NM: negative medium, Z: zero, PM: positive medium, PL: positive large, N: negative, and P: positive. The fuzzy rules used are of the Mamdani type shown in Table 1. It is noteworthy that Mamdani rules used in this research have been obtained by trial and error.

Table 1. Fuzzy rules based on fuzzy system inputs and output

	w1	$\frac{dw1}{dt}$		
		P	N	ZE
G1	PL	PL	PL	PL
	PM	PL	PS	PM
	PS	PM	ZE	PS
	ZE	PM	NM	ZE
	NS	ZE	NM	NS
	NM	NS	NL	NM
	NL	NM	NL	NL
	w2	$\frac{dw2}{dt}$		
		P	N	ZE
G2	PL	PL	PL	PL
	PM	PL	PS	PM
	PS	PM	ZE	PS
	ZE	PM	NM	ZE
	NS	ZE	NM	NS
	NM	NS	NL	NM
	NL	NM	NL	NL

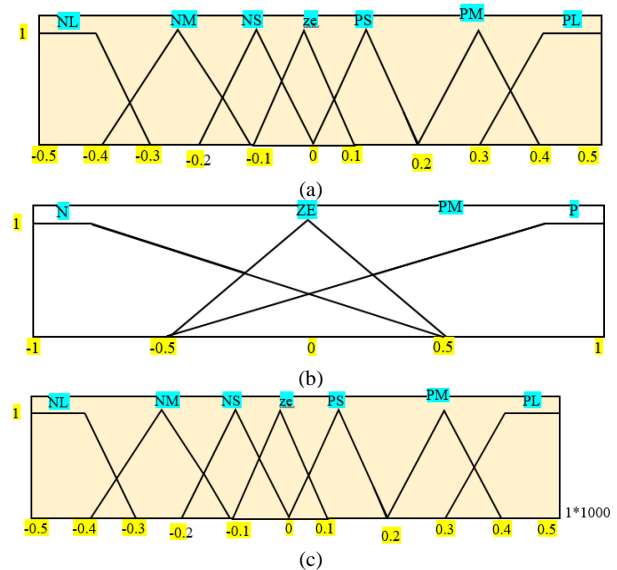


Fig.6. inputs and output membership functions: (a)- speed of generators, (b)- speed change of generators, (c)- out put of fuzzy controller

As mentioned, the fuzzy rules are of the Mamdani type.

The rules in terms of input parameters, i.e., the angular velocity of synchronous generators and, variations are outlined as shown in Table 1. According to Table 1, for instance, if $w1$ is NS, and $\frac{dw1}{dt}$ is N, then the output is NM. Finally, the output of the fuzzy system must be converted to a crisp number. As mentioned, there are several defuzzification methods available. Centroid technique is one of the commonly used defuzzification methods, is used in this research. In this method, the control signal is:

$$\Delta U(K) = \frac{\sum_{i=1}^n M_i T_i}{\sum_{i=1}^n T_i} \quad (3)$$

In Eq. (3), where M_i is the membership grade and T_i is the membership function singleton position.

5. RESULT OF TIME-DOMAIN SIMULATION

Modified version of the IEEE second benchmark model including DFIG- based wind farms was used to evaluate the proposed controller, and MATLAB/Simulink software was applied for simulating the time of the studied system. As mentioned before, the percentage of compensation of the transmission line is considered as one of the influential factors in SSR fluctuations, which increases with the percentage of compensation of the system towards instability. In general, the simulation is done in three parts. Initially, the system operates without auxiliary control and at 75% compensation (x_c/x_l), and at moment $t = 1$ seconds, a three-phase fault occurs at bus j , which disappears at moment $t = 1.0025$ seconds. Figure 7 shows the torque of the steam turbine rotor in different parts, which is unstable in the percentage of compensation. In this research, the torque of the different parts of the steam turbine of both generators is in per- unit.

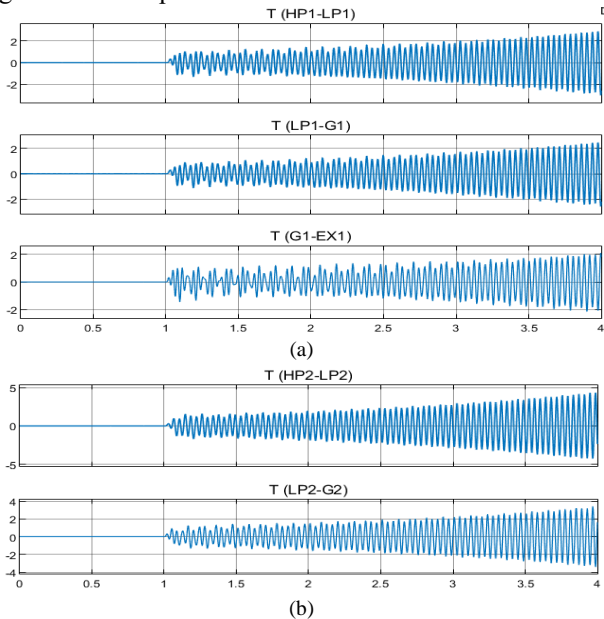


Fig. 7. (a): torque T (HP1-LP1), T (LP1-G1), T (G1-EX1) in steam turbine of G1, (b): T (HP2-LP2), T (LP2-G2) in steam turbine of G2 without damping

In the following, the application of fuzzy controller designed based on WAMS to dampen SSR fluctuations in two ideal modes and in the presence of time delays.

5.1. Wide-Area Fuzzy Controller without Time Delay

This part of the simulation shows the application of fuzzy controller to the studied system in case the delays caused by the measured PMU signals are ignored. As shown in Figure 8, SSR fluctuations damped by applying a controller to the stator voltage control loop in the GSC. With the 42 fuzzy rules in Table 1, and receiving the controller inputs, which is the same as angular velocity, and variations of generators synchronous from the PMU, the membership functions of Figure 8 will be quenched by the SSR fluctuations shown in Figure 8. According to Figure 8, in the case where the compensation percentage is 75 and the system is unstable, in the first second of the simulation a three-phase fault occurs at bus j , which disappears at moment $t = 1.0025$ seconds and by applying a fuzzy controller, the oscillations will be damped.

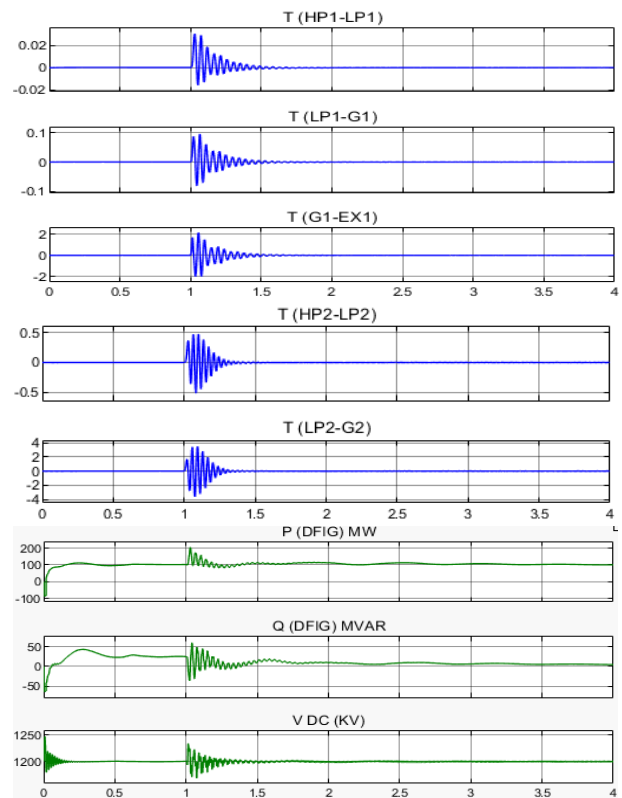


Fig. 8. Damping of SSR oscillation in synchronous generation and DFIG ignoring time delay

In Figure 8, SSR fluctuations damped by applying a controller to the stator voltage control loop in the GSC. With the 42 fuzzy rules in Table 1, and receiving the controller inputs, which is the same as angular velocity, and variations of generators synchronous from the PMU, the membership functions of Figure 8 will be

quenched by the SSR fluctuations shown in Figure 8. According to Figure 8, in the case where the compensation percentage is 75 and the system is unstable, in the first second of the simulation a three-phase fault occurs at bus *j*, which disappears at moment $t = 1.0025$ seconds and by applying a fuzzy controller, the oscillations will be damped.

5.2. Wide-Area Fuzzy Controller with Time Delay

In the previous section, WAMS-based fuzzy controller simulations were performed in which the latencies due to PMU measurement signals were ignored. In practice, these time delays in sending signals to the controller cannot be ignored because delays are inevitable in telecommunication systems. According to reference [31], these delays are classified as Table 2, therefore if these delays are ignored, system instability, as shown in Figure 9. Figure 9 shows the state that the measurement signals applied to the wide-area fuzzy controller have a delay of 350 ms and the actions of the controller in the first second have caused system instability and failed to dampen the system.

Table 2. Time delay of communication links

Communication link	Associated delay (ms)
Fiber- optic cables	100-150
Digital microwave link	100-150
PLC	150-350
Telephone Lines	200-350
Satellite link	500-700

Table 3. Rule-based on wide-area fuzzy controller with time delay

Time delay	w1	$\frac{dw1}{dt}$							
		PL	PM	PS	ZE	NS	NM	NL	
M	P	PS	NL	PL	PM	PM	NM	NM	PM
	N	NL	ZE	PM	NL	NS	NM	PS	
	ZE	NS	PS	NM	ZE	PL	NM	NL	
L	P	ZE	PM	PL	NM	NL	NM	PM	
	N	PL	ZE	NM	PM	PM	PS	NM	
	ZE	PS	NL	ZE	PL	NM	ZE	PL	

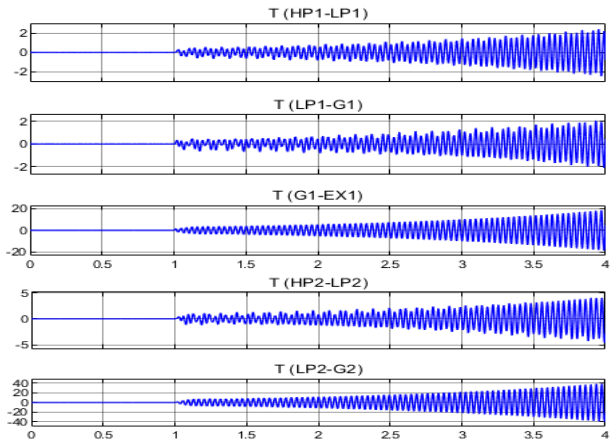


Fig. 9. SSR osilation in synchronous generation with wide-area fuzzy controller and time delay equal to 350 ms

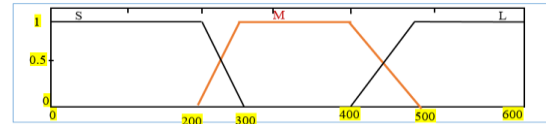


Fig. 10. Membership functions of the latency variable for wide-area fuzzy controller with time delay

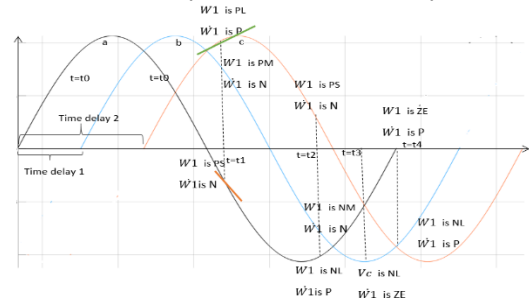


Fig. 11. Time delay signal of w1

The membership functions associated with the fifth input are given in Figure 12. As it can be seen, the amount of latencies due to measuring PMU signals is divided into three intervals S: small, M: medium, and L: large. Thus, three membership functions are introduced for the latency. To apply this fuzzy input to the fuzzy system, the fuzzy rules of Table 1 are changed, the cause of which is well illustrated in Figure 11. Figure 11 shows the angular velocity of G1 in three modes without delay (a), medium delay (b), and long delay (c), its dimensions can be in terms of per- unit.

Table 4. The value of Coefficients k_{d1} , and k_{d2}

Methods of optimization	k_{d1}	k_{d2}
PSO	0.64	0.38
ICA	0.72	0.57

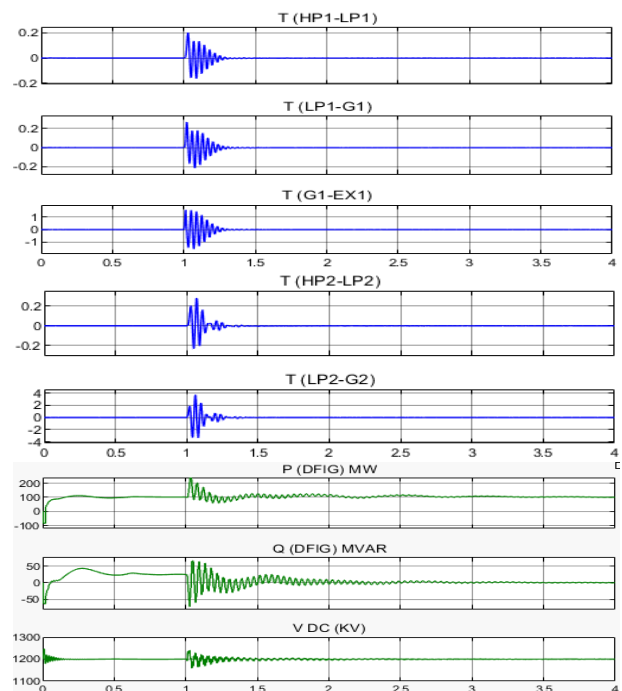


Fig. 12. Damping of SSR oscillation in synchronous generations and DFIG with wide-area fuzzy controller including time delay equal to 400 ms

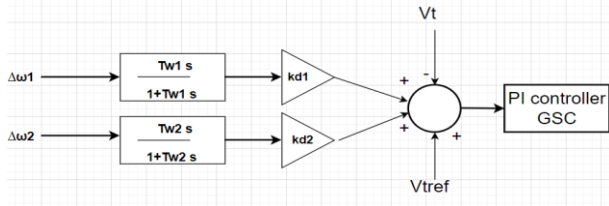


Fig. 13. Structure of damping controller with optimization methods

Consider the moment $t = t_1$ as an example. At this point, the main signal is the no-delay input of W1 is PS and $(W1)'$ is N, which according to Table 3 will be the output value of the fuzzy controller equal to ZE. While, at this moment, if the medium delay is (M: Time delay 1), thus, the fuzzy rule in this delay as W1 is PM and $(W1)'$ is N, which should be the output of system the ZE. In addition, at this time, if the delay are large, is (L: Time delay 2), the fuzzy rule in this delay as W1 is PL and $(W1)'$ is P, which must be the output of the fuzzy system in this delay is also ZE. Similarly, other modified fuzzy rules are shown by considering the delays table 3. Similarly, Fuzzy rules to apply W2 Generator G2 is repeated as in Table 3. By changing the fuzzy rules, which are modeled taking into account the delays caused by PMU measurement signals, the simulation of the studied system with two-time delay of 400 milliseconds is shown in Figures 12. According to this figure, it can be seen that the fuzzy controller has been able to dampen the fluctuations caused by SSR by considering the changes in fuzzy rules.

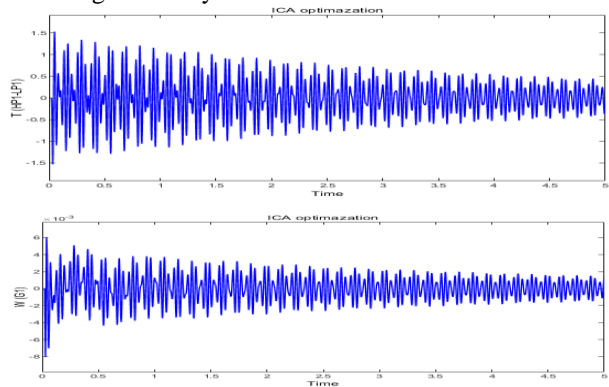


Fig. 14. Damping of SSR with ICA method

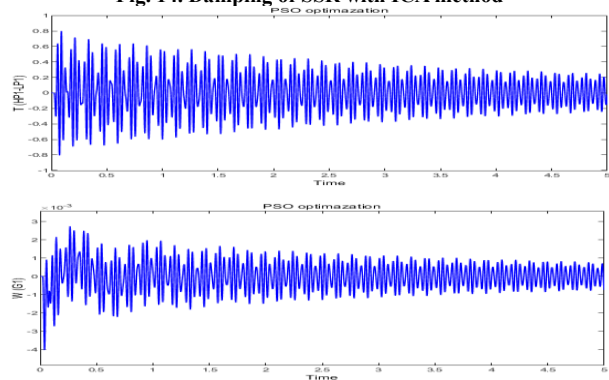


Fig. 15. Damping of SSR with PSO method

To compare the results of proposed method with the methods that have been worked based on optimization metaheuristic such as PSO and ICA, as mentioned in various references, which considering the control structure of figure 13. It is possible to optimize its parameters by optimizing the objective function Eq. (4) with the PSO and ICA optimization methods.

$$\text{Objective Function} = \min(f) \tag{4}$$

$$f = \int_{t=0}^{t=t_{sim}} t |\Delta\omega_1 + \Delta\omega_2| dt$$

In Eq. (4), t_{sim} represents the simulation time, $\Delta\omega_1$ and $\Delta\omega_2$ the angular velocity variations of the synchronous generators. To calculate the objective function, the time domain of the system model must be simulated with respect to all saturation constraints. The permissible limit k_{d1} , and k_{d2} is between zero, and one. Table 4 shows the results of optimization of Objective Function Eq. (3) by both PSO and ICA methods. In addition, Figures 16, and 17 shows the angular velocity variations of generators with PSO and ICA algorithms. In addition, comparison of Figures 14 and 15 with Figure 12 shows that the proposed WAMS-based fuzzy controller method is faster. Another important point in the method proposed in this paper is no need to adjustment of parameters at each level compensates for transmission lines.

6. CONCLUSION

In this paper, was used a new method for damping SSR fluctuations in power systems including DFIG-based wind farms linked to series capacitive compensated transmission lines. . No need to adjust the parameters of the controller as well as working at a high level of compensation, namely seventy-five% and use of WAMS with considering time delay by the PMU measurement, and utility DFIG-based wind farms including power systems is the main feature of this controller. In addition, delays due to communication signals were shown to be important in using WAMS. If these delays are ignored, it causes system instability. The effectiveness of this controller in damping of SSR fluctuations and compared with the methods that have been worked based on optimization metaheuristic such as PSO and ICA has been demonstrated by time simulation using software MATLAB/Simulink on a modified version of the IEEE second benchmark model including DFIG-based wind farms.

Appendix A
Systems parameters:

Table A1. Parameter of DFIG-based wind farms

Base Power	2 MW	100 MW
Based voltage (VLL)	690 V	690 V
Xls	0.09231	0.09231
Xlr	0.09955	0.09955
Rs	0.00488	0.00488
XM	3.95279	3.95279
Xtg	0.3 (0.189 mH)	0.3 (0.189/50 mH)
DC-link base voltage	1200 V	1200 V
DC-link capacitor	14000 μ F	50*14000 μ F

Transmission lines:

$$R_L = 0.02 \text{ pu} \quad X_T = 0.14 \text{ pu}$$

$$X_L = 0.05 \text{ pu} \quad X_{\text{sys}} = 0.06 \text{ pu},$$

Transformer ratio: 26/539 kV

Shaft parameters:

$$H_{HP} = 0.092897, H_{IP} = 0.155589, H_{LPA} = 0.858670,$$

$$H_{LPB} = 0.884215, H_{GEN} = 0.868495$$

$$H_{EXC} = 0.0342165, K_{HP-IP} = 19.303 \text{ pu / rad},$$

$$K_{IP-LPA} = 34.929 \text{ pu / rad}, K_{LPA-LPB} = 52.038 \text{ pu / rad},$$

$$K_{LPB-GEN} = 70.858 \text{ pu / rad}, K_{GEN-EXC} = 2.82 \text{ pu / rad}.$$

REFERENCES

- [1] X. Lie, and P. Cartwright, "Direct active and reactive power control of DFIG for wind energy generation", *IEEE Trans. Energy Conv.*, vol. 21, pp. 750-758, 2006.
- [2] P. Richard et al., "Integrating large wind farms into weak power grids with long transmission lines", *CES/IEEE 5th Int. Power Electron. Motion Control Conf.*, 2006.
- [3] F. Lingling, C. Zhu, Z. Miao, "Modal analysis of a DFIG-based wind farm interfaced with a series compensated network", *IEEE Trans. Energy Conv.*, vol. 26, pp. 1010-20, 2011.
- [4] X. Lie, and P. Cartwright, "Direct active and reactive power control of DFIG for wind energy generation", *IEEE Trans. Energy Conv.*, vol. 21, pp. 750-758, 2006.
- [5] H. Mohammadpour, and E. Santi, "Optimal adaptive sub-synchronous resonance damping controller for a series-compensated doubly-fed induction generator-based wind farm", *IET Renew. Power Gener.*, vol. 9, pp. 669-681, 2009.
- [6] Y. Cheng et al., "Sub-synchronous interaction in Wind Power Plants-part II: An ergot case study", *IEEE Power Energy Soc. Gen. Meet.*, 2012.
- [7] F. Lingling, R. Kavasseri, and Z. Lee, "Modeling of DFIG-based wind farms for SSR analysis", *IEEE Trans. Power Del.*, vol. 25, pp. 2073-2082, 2011.
- [8] W. Liang, X. Xie, and Q. Jiang "Mitigation of multimodal subsynchronous resonance via controlled injection of supersynchronous and subsynchronous currents", *IEEE Trans. Power Syst.*, vol. 29 pp.1335-1344, 2013.
- [9] X. Hailian, and M. de Oliveira, "Mitigation of SSR in presence of wind power and series compensation by SVC", *Int. Conf. Power Syst. Tech.*, 2014.
- [10] T. Arantxa, G. Tapia, J. Xabier Ostolaza, "Modeling and control of a wind turbine driven doubly fed induction generator", *IEEE Trans. Energy Conv.*, vol. 18, pp. 194-204, 2003.
- [11] X. Lie, and Y. Wang, "Dynamic modeling and control of DFIG-based wind turbines under unbalanced network conditions", *IEEE Trans. Power Syst.*, vol. 22, pp. 314-323, 2007.
- [12] F. Michael et al., "A power system stabilizer for DFIG-based wind generation", *IEEE Trans. Power Syst.*, vol. 21, pp. 763-772, 2006.
- [13] B. Jan, E. Muljadi, "The wind farm aggregation impact on power quality", *IECON Annual Conf. IEEE Ind. Electron.*, 2006.
- [14] D. Fateh, A. Birjandi, M. Guerrero, "A subsynchronous resonance prevention for DFIG-based wind farms", *Turkish J. Electr. Eng. Comput. Sci.*, vol. 28, pp. 2670-2685, 2020.
- [15] L. Huakun et al., "Quantitative SSR analysis of series-compensated DFIG-based wind farms using aggregated RLC circuit model", *IEEE Trans. Power Syst.*, vol. 32, pp. 474-483, 2016.
- [16] F. Lingling, and Z. Miao, "Mitigating SSR using DFIG-based wind generation", *IEEE Trans. Sustain. Energy*, vol. 3, pp. 349-358, 2012.
- [17] H. Mohammadpour et al., "SSR damping in wind farms using observed-state feedback control of DFIG converters", *Electr. Power Syst. Res.*, vol. 123, pp. 57-66, 2015.
- [18] F. Sherif et al., "Utilizing DFIG-based wind farms for damping subsynchronous resonance in nearby turbine-generators", *IEEE Trans. Power Syst.*, vol. 28, pp. 452-459, 2013.
- [19] X. Zhang, X. Xie, H. Liu, "Mitigation of sub-synchronous control interaction in wind power systems with GA-SA tuned damping controller", *IFAC-Papers On Line*, vol. 50, pp. 8740-8745, 2017.
- [20] W. Yun et al., "H ∞ current damping control of DFIG based wind farm for sub-synchronous control interaction mitigation", *Int. J. Electr. Power Energy Syst.*, vol. 98, pp. 509-519, 2018.
- [21] L. Huakun et al., "Mitigation of SSR by embedding subsynchronous notch filters into DFIG converter controllers", *IET Gen. Transm. Distrib.*, vol. 11, pp. 2888-2896, 2017.
- [22] X. Hailian et al., "Subsynchronous resonance characteristics in presence of doubly-fed induction generator and series compensation and mitigation of subsynchronous resonance by proper control of series capacitor", *IET Renew. Power Gen.*, vol. 8, pp. 411-421, 2014.
- [23] I. Garth, A. Jindal, L. Isaacs, "Sub-synchronous control interactions between type 3 wind turbines and series compensated AC transmission systems", *IEEE Power Energy Soc. Gen. Meet.*, 2011.
- [24] J. Yingzong et al., "Analysis and mitigation of subsynchronous resonance for doubly fed induction generator under VSG control", *Energies*, vol. 13, pp. 1582- 1588, 2020.
- [25] D. Raju et al., "Mitigation of subsynchronous resonance with fractional-order PI based UPFC controller", *Mech. Syst. Signal Proc.*, vol. 85, pp. 698-715, 2017.
- [26] D. Raju et al., "Fractional-order PI based STATCOM and UPFC controller to diminish subsynchronous resonance", *Springer Plus*, vol. 5, pp. 1-20, 2018.
- [27] D. Raju et al., "Improved control strategy for subsynchronous resonance mitigation with fractional-order pi controller", *Int. J. Emerging Electr. Power Syst.*, vol. 17, pp. 683-692, 2018.
- [28] K. Raju et al., "Effect of SSSC-based SSR controller on the performance of distance relay and adaptive approach using synchronized measurement", *Int. Trans. Electr. Energy Syst.*, vol. 28, pp. 2620-2628, 2017
- [29] V. Subinay et al., "Implementation of PLL algorithm in DFIG based wind turbine connected to utility grid", *Second Int. Conf. Inventive Res. Comput. Appl.*, 2020.